INVESTIGATION OF THE DEVELOPMENT OF FUEL ASSEMBLY BOW IN RINGHALS 3 AND 4

P. GABRIELSSON, D. SCHRIRE, E. SUVDANTSETSEG
Vattenfall Nuclear Fuel AB
SE-169 92 Stockholm, Sweden
petter.gabrielsson@vattenfall.com,

M. MALMBERG
Ringhals AB
SE-432 85 Väröbacka, Sweden

ABSTRACT

Fuel assembly bow has been increasing in Ringhals 3 and 4 since 2012/2013. To get a better understanding of this development a new measurement device was taken in use in 2017 to facilitate out-of-core assembly bow measurements of all assemblies, “on-line” after unloading. A new database of bow data and correlated parameters was built and analysed. The analysis reveals that irrespective of the loading pattern a similar bow pattern now develops in the core at the end of the cycle. A situation close to equilibrium appears to have been reached in Ringhals 3, with a maximum bow, on free-standing assemblies, in the x- or y-direction of around 10 mm. The predominant bow shape has changed from S to C. This is shown to have a major impact on the radial power peaking factor, which must be accounted for in the safety evaluation. As a countermeasure, fuel designs with significantly increased lateral stiffness will be introduced.

1. Introduction

Operating experience of PWR’s has shown that collective fuel assembly bow may challenge both safety margins and availability, due to problems with fuel handling, control rod insertion and core power redistribution.

In Vattenfall’s three PWR’s at the Ringhals site, assembly bow has been a major concern since the Incomplete Rod Insertion event in Ringhals 4 in 1994 [1]. Safety assessments for assembly bow have been performed for all 3 reactors and the development of the bow has been monitored annually with visual measurements of around 20 carefully selected assemblies during the outage. Several fuel design improvements have been implemented – to reduce fuel assembly growth, reduce hold-down forces and improve guide thimble creep strength and lateral stiffness – and this has gradually led to reduced bow amplitudes down to relatively insignificant levels in 2012/2013. However in the following years up to 2017, bow measurements in both Ringhals 3 and 4 have again showed increasing bow amplitudes. A comprehensive investigation has therefore been undertaken by Vattenfall in order to identify the causes, anticipate further development, identify relevant mitigating actions and ensure continued safe operation and high availability of the reactors.

Ringhals 3 and 4 are Westinghouse 3-loop reactors with 157 12 ft assemblies with 17x17 fuel rod array. The units were commissioned in 1981 and 1983 respectively, with an original core thermal power output of 2775 MW. Both units were in later years uprated after steam generator and turbine replacements and are now operated at 3135 and 3292 MW, respectively. Annual cycles and low leakage loading patterns are employed.

2. Fuel assembly bow measurements

2.1. Development of the fuel assembly bow measurement technique

A first step to strengthen the surveillance of the fuel assembly bow was taken during the outage of Ringhals 3 in 2016 when for the first time the full core was measured. The bow measurement was performed by visual measurement of the grid displacement at grids 2 to 7, relative to the reference frame defined by the end grids (grids 1 and 8), at each face of the grids. Full core measurements had never been done at Ringhals before since they are very time consuming. The measurement of an assembly takes approximately 30 minutes and the uncertainty is estimated to be ±1.0 mm.

The availability of full core bow measurement data led to a new understanding of the situation in the core. Moreover, full core measurement data provides completely new possibilities for accurate analysis of the in-core water gaps and the future bow development.

Based on the results of the full core measurement in 2016 it was decided to procure a new measurement system allowing for quicker and more accurate measurements during outage, “on-line” without impact on outage length.

2.2. MABEMA Fuel 3D

The Mabema Fuel 3D system is designed to measure the geometry of each fuel bundle ”on-line” to monitor the fuel assembly bow trend. The system consists of a vertical rod with eight laser triangulation systems placed vertically at pre-selected positions close to the structural spacer grids. Each laser triangulation system consists of a laser emitter and a camera.

The system measures the fuel assembly while it is hanging from the fuel handling crane. The fuel bundle is placed in front of the Fuel 3D system for a few seconds while the Mabema Fuel 3D system measures the fuel by means of laser triangulation. The angle between the laser emitter and the camera generates a planar projection of the fuel assembly. The eight triangulation systems generate a total of eight projected planes.

The bow at each of the six projected planes placed between the top and bottom planes are defined as the distance between the corner rod and a projected line drawn through the corner rods of the top and bottom projection. When a corner rod has been measured, the fuel bundle is rotated 90 degrees and measured once more. This process is repeated until all four sides have been measured. Displacements in x- and y-direction are then given in four sets of data for six axial positions. For each axial position the average value is used for downstream evaluations.

2.3. Fuel assembly bow in free-standing vs hanging condition

Since the visual bow measurements have been performed on fuel assemblies standing in the refuelling pool and the Mabema Fuel 3D measurements are performed on fuel assemblies hanging freely in the fuel handling crane, the bow amplitudes measured in hanging condition need to be translated into the corresponding amplitudes in standing condition, to allow for comparison with historical bow measurement data and for direct translation to in-core conditions.

Unfortunately it is not practicable to use the Mabema Fuel 3D on seated fuel assemblies to determine the difference in bow compared to hanging assemblies. Instead Ringhals performed measurements using both techniques on a selection of assemblies – visual measurement of the assembly in standing condition and laser measurement of the assembly in hanging condition. The measurements show around 20% higher bow amplitudes on standing assemblies than on hanging assemblies, see Figure 1.

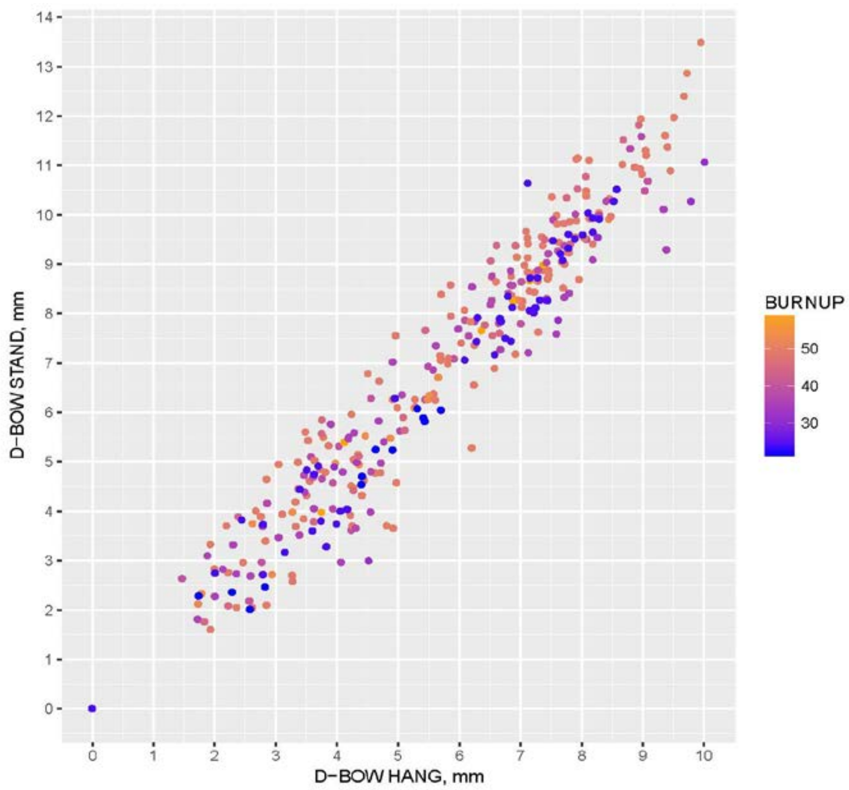

Figure 1. Diagonal bow (D-bow) at all spacer grid levels, measured on assemblies in standing and hanging condition.

It is assumed that the change in displacement of each grid is primarily dependent on bow amplitude, grid position, bow shape and lateral stiffness - which is fuel design and burnup dependent. Based on the measurement data from assemblies measured both when standing and when hanging a correlation for the translation between the two states was developed. The correlation is only applicable for the fuel design and C-shaped bow with amplitudes covered by the database. The only correlation parameters are grid position and measured displacement per grid position. The database gave no evidence of a significant burnup dependence and the correlation could not be significantly improved through introduction of this parameter.

The correlation in general behaves well, with a majority of predictions within ±0.5 mm from measured data, but there are also some outliers that are not well understood. Part of this could be an effect of combined measurement uncertainties. However, it appears that the correlation becomes more uncertain with higher burnup, but the influence of burnup is not systematic so it doesn't help to include burnup as a correlated parameter. It is possible that the burnup effect is rather an effect of bow history than an effect of reduced lateral stiffness. To improve the correlation with theoretical models to take this into account therefore seems challenging.

In principle, a free-standing assembly should have a larger bow amplitude than a hanging assembly, since the weight of the upper part of the assembly acts as an axial compressive load that tends to promote elastic buckling. However, friction between spacer grids and fuel rods affects the elastic bow deformation. The friction effect is history dependent, including the horizontal transportation of the assemblies in the fuel transfer system.

Due to the remaining uncertainty in the translation from hanging to standing bow, the assemblies with the highest bow in hanging condition will continue to be measured also in seated condition with the visual method during coming outages. Additional visual measurements would also be required if bow amplitudes continue to increase beyond the existing database, when new fuel designs with another (higher) lateral stiffness are introduced or if the bow shape would change (which is not expected).

2.4. Fuel assembly bow database

Until recently, the fuel assembly bow measurements were mainly used to follow the development of measured mean and maximum absolute fuel assembly bow in x- or y-direction. To get more information out of the measurements, and possibly improve the understanding of the new bow trend, it was necessary to build a new database connecting fuel assembly data, operating data, bow data and measurement data. This database then enables the study of trends in many different bow related parameters and to correlate these observed trends to other relevant parameters in order to try to strengthen or dismiss suspected drivers for the bow development.

3. Investigation of fuel assembly bow trends, causes and remedies

3.1. Trends

Analysis of the bow data shows that the increase in bow amplitudes has coincided with a marked transition from S- to C-bow and a 180 degree change of dominant bow direction, from South-East to North-West direction. This is especially clear in Ringhals 4, see Figure 2.

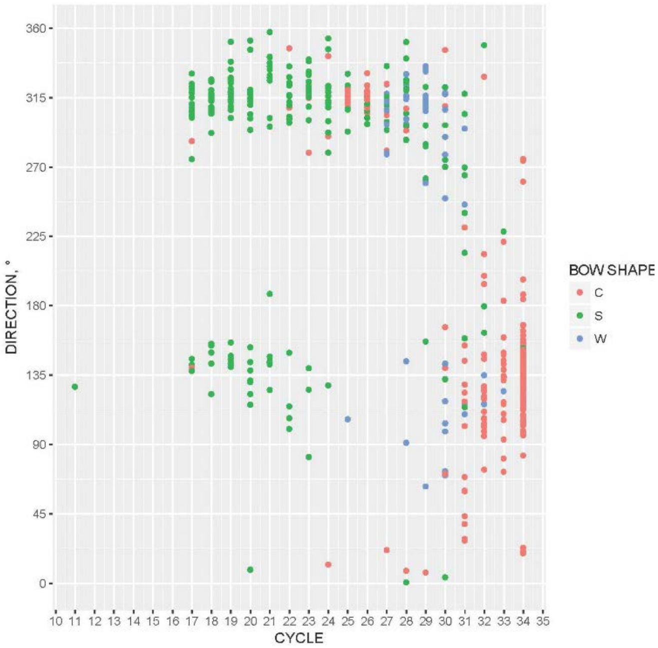

Figure 2. Cycle-by-cycle development of dominant bow direction and bow shapes of all measured assemblies in Ringhals 4.

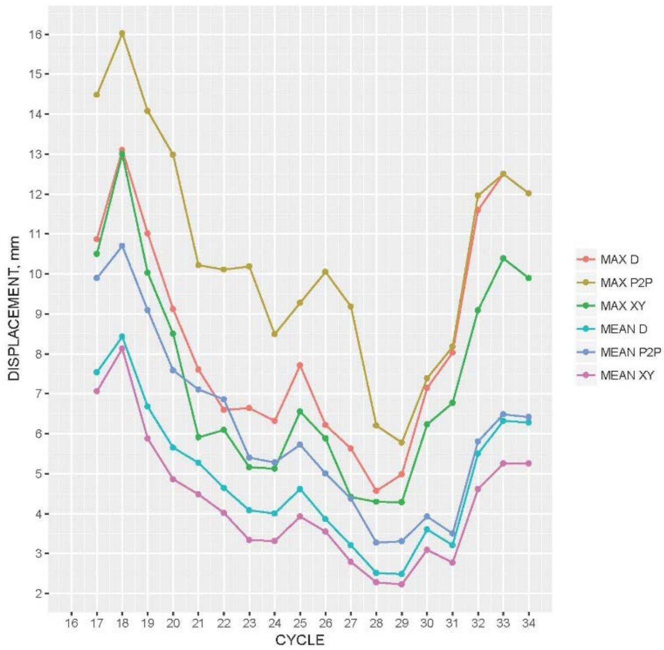

Figure 3. Cycle-by-cycle development of mean and max diagonal bow, peak-to-peak bow and x- or y-bow of all measured assemblies in Ringhals 3. (Fuel 3D data only in Cycle 34.) .

The bow amplitudes have increased quickly year-by-year since 2013, but this development came to a halt in Ringhals 3 in 2017, see Figure 3. The development in Ringhals 4 is similar but lags by 1-2 years.

The study of the full core bow patterns reveals that a well-ordered, “smooth” and symmetric bow pattern with general bow direction towards North-West is recurring at the end of cycle (EOC), see Figure 4-5. The EOC bow amplitude and bow direction of individual assemblies seem to be more dependent on the position in the core/bow pattern, than on other factors including the loading pattern and the number of fresh assemblies.

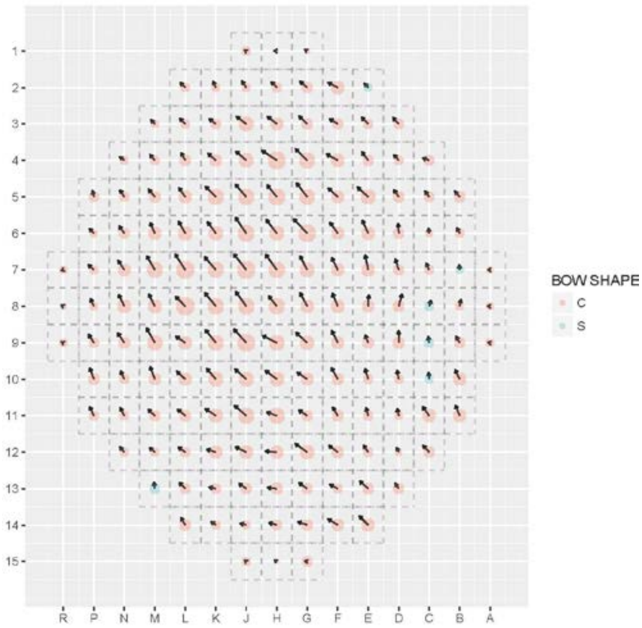

Figure 4. Ringhals 3 at end of cycle 34 middle of the core (spacer grid 5) bow vectors and circles denoting bow shape and magnitude of cumulative curvature.

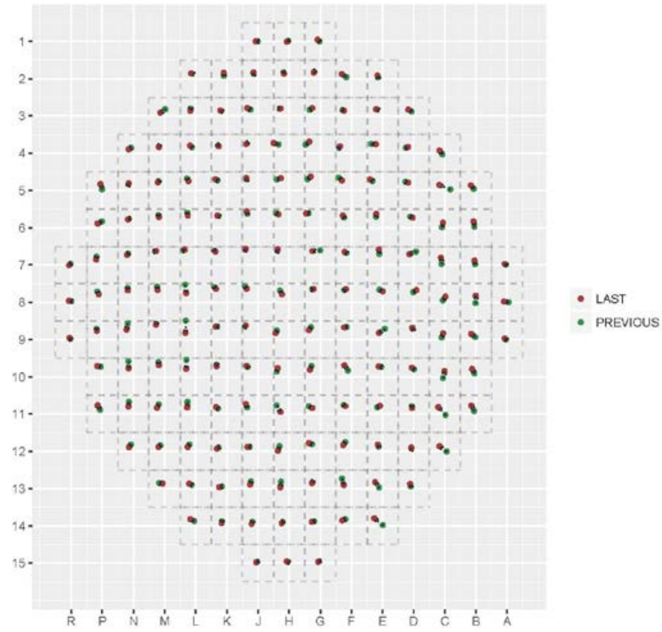

Figure 5. Comparison of the point of bow vector “tips” from measurements in Ringhals 3 EOC34 and EOC33 per core position. In most positions the EOC bow vector after the latest cycle is similar to after the previous cycle.

The in-core quadrant power tilt has increased in the latest cycles, with an increase in power in the South-East quadrant and decrease in power in the North-West quadrant. This is consistent with the opening up of water gaps between bowed and fresh assemblies in the South-East, and closing of water gaps in the North-West, at beginning of cycle (BOC). So far the power tilt is below 2%.

3.2. Causes

The transition from S- to C-bow is seen as evidence that axial compressive loads are no longer the main driver of bow, but rather the lateral loads from neighbouring, already bowed fuel assemblies and flow forces. Thus, the reload fuel assemblies were concluded to have insufficient lateral stiffness for the forces exerted on them in Ringhals 3 and 4.

The reason why the C-shaped bow developed to the North-West in both Ringhals 3 and 4, while S-shaped bow was more accentuated to the South-East, is not fully understood. However, in the last cycles with S-bow the amplitudes in both directions was relatively small, so other factors could more easily become influential. One such factor that was considered is the reactor coolant pump start-up sequence which would be more likely to initiate bow towards North-East. The flow asymmetries between the loops during normal, full power operation are on the other hand judged to be too small to have an important effect on the lateral flow forces.

Analysis of the bow data, in search for explanations for the increasing bow trend, lead to the conclusion that the main reason for the development of strong C-bows was the introduction of a new reload fuel design in 2011-2012. The delayed bow development in Ringhals 4 is consistent with a later and slower introduction of this fuel product.

No other strong correlations to the bow development were found. However, cycle length is also influential - the biggest increases of bow over a cycle have coincided with longer cycles. For long cycles more fresh fuel assemblies are required, which initially helps to reduce the mean bow amplitude at BOC, but for the current conditions in Ringhals 3 and 4 it appears that this positive effect is outweighed by the negative effect on bow when lateral loads are allowed to work on the assemblies for a longer period of time before reshuffling.

The recurrence of the same bow pattern at EOC is partly attributed to the boundary condition imposed by the core baffle, but could hardly occur without the additional aid of lateral flow forces. This conclusion is supported by the fact that fuel vendor assembly bow analyses were able to capture the general bow development but not the well-ordered symmetric bow pattern, when lateral flow forces were unknown and set to zero.

Recurring bow patterns have been reported from other reactors that were operated with an equilibrium loading pattern [2]. The example from Ringhals 3 and 4 shows that the same kind of bow pattern also develops for reactors operated with variable cycle lengths and loading patterns. The loading pattern is of little importance for the bow pattern at EOC. This implies that the higher lateral stiffness of fresh fuel assemblies is reduced to a level closer to that of the already burnt assemblies already during the first cycle. Therefore at EOC little or none of the straightening effect of the fresh fuel assemblies remain.

The highest bow amplitudes are so far situated to the North-West of the core center. This is consistent with the theory that lateral flow forces work from the core center and radially outwards, which potentially increases lateral loads in the North-West and reduces lateral loads in the South-East. Analysis of resulting water gaps at EOC reveals that most gaps are already closed in the North-West, which leaves little potential for further increase of bow in this part of the core. Higher bow amplitudes could develop in the South-East, but this development may be counteracted by lateral flow forces. This might explain why bow is not increasing and that an equilibrium situation instead seems to have been reached for the bow amplitudes in Ringhals 3, as seen in Figure 2.

3.3. Remedies

The following remedies have so far been identified and implemented in Ringhals 3 and 4:

- In cooperation with the reload fuel vendor, design improvements were conceived and qualified [3]. The modified product will have improved lateral stiffness of the fuel assembly and skeleton, as well as reduced axial hold-down forces. First reloads of the modified product will be loaded in both units in 2018. However, based on previous experience the positive effects on bow amplitudes may not be seen until the core is dominated by the modified product, which will probably take 3 reloads.

- As a precaution, reactor coolant pump startup sequences with the potential to induce stronger lateral flow forces towards the North-West, are now avoided.

- In order to avoid increased bow amplitudes in the South-East, where there is plenty of room for it, shuffling of the most bowed assemblies in North-West to South-East will be avoided when possible.

- In order to reduce the mean bow amplitude at BOC, a checker-board type of loading pattern – with alternating fresh and burnt assemblies – is recommended. This is first of all thought to be efficient to reduce in-core quadrant power tilt at BOC, since the core will be efficiently straightened and water gaps will be reduced and present both in South-East and North-West. With a reload fuel design with higher skeleton lateral stiffness, the positive initial straightening of the core at BOC, is expected to remain also at EOC, to a higher degree.

4. Fuel assembly bow acceptance criteria

4.1. Control rod insertion

The most acute safety consequence of fuel assembly bow would be an Incomplete Rod Insertion during reactor trip. However, operating experience shows that this event has only occurred in fuel assemblies with an S-shaped bow. The development of C-shaped bow in Ringhals 3 and 4, albeit with increasing amplitudes, is therefore benign from the control rod insertion perspective. Based on previous operating experience, including the Incomplete Rod Insertion event in Ringhals 4 1994, Vattenfall introduced new conservative acceptance criteria to verify control rod insertability:

- Maximum peak-to-peak bow of an S-shaped fuel assembly < 15 mm
- Maximum cumulative curvature of a fuel assembly of any shape < 35
  (The cumulative curvature is the sum of curvatures, where the curvature at each spacer grid is calculated from the angle between the two adjacent spacer spans.)

In 2017 in Ringhals 3 the maximum peak-to-peak bow of an S-shaped fuel assembly was 4.5 mm (<< 15) and the maximum accumulated curvature was 15 (<< 35). For the fuel assembly with Incomplete Rod Insertion in Ringhals 4 in 1994 the corresponding values were 22 mm and 98.

In addition to this, control rod drop times are measured at BOC and EOC and criteria are defined both for allowed deviation from established normal values for each control rod position and for the allowed drop time development during a cycle.

Finally, standard criteria are employed for measured control rod friction in the guide thimbles. All control rods are measured at BOC and core positions exhibiting a prolonged drop time are measured also at EOC.

Fuel assemblies for which drop time or friction criteria are violated shall not be placed in control rod position in the following cycle, unless fuel assembly bow measurements of the assembly show that bow can be ruled out as a cause for the violation.

No or very little effect of fuel assembly bow can be seen on control rod drop times and friction. This is also as expected with C-shaped bow.

It is concluded that rod insertion is not a main concern for the current assembly bow in Ringhals 3 and 4. This statement might be general for all 12-ft reactors with modern fuel designs with a low and controlled growth and optimized hold-down forces, for which S-shaped bow is unlikely to occur. The main concern with C-shaped fuel assembly bow is instead the water gaps and power redistribution effects.

4.2. Power redistribution

As the fuel assemblies bow, the gaps between assemblies change from their nominal, uniform configuration. This causes a change in the local neutron moderation and thereby the power distribution. This effect is not reflected in the plant core model which assumes a uniform, nominal gap distribution. Instead, in order to take this power redistribution into account, generic water gap analyses have been performed to determine assembly bow peaking factor penalties to be used for the reload safety verification. The applicable bow acceptance criteria in order to verify power redistribution effects are then based on the continued validity of the water gap analyses.

For Ringhals 3 and 4, the water gaps analyses covered out-of-core fuel assembly bow amplitudes up to 20 mm in x- or y-direction [4]. However, since the analyses were performed based on older bow measurements from Ringhals 3 and 4, they only covered S-shaped bow.

With S-shaped bow an assembly side will see an increase in water gap over only part of the assembly height followed by a nominal gap or gap reduction over the remainder of the height. With C-shaped bow on the other hand, most of the height of an assembly side will see an increase in gap and hence moderation. This means that the integral rod power, FΔH, is much more affected by C-shaped bow than by S-shaped bow. This led to the conclusion that the water gap analyses had to be revised for the new bow situation in Ringhals 3 and 4.

5. Impact of enhanced water gaps

5.1. Neutronic water gap penalties

The effect of improved moderation can be large in the rows of fuel rods on either side of an enhanced gap, but quickly decreases towards the interior of the assembly. The peripheral fuel rods may then well become leading in power in the assembly, whereas under nominal conditions inner fuel rods would be leading in power. The neutronic FΔH peaking factor penalty is based on the ratio between leading rod power with enhanced water gaps and leading rod power with nominal gaps. So even if the increase in rod power in outer rods may be high (eg. >20%), the percent increase in the leading rod power will be more limited (eg. <10%), but still high enough to be a concern.

In order to encompass an increased neutronic FΔH peaking factor penalty without violation of the FΔH safety analysis limit, the best estimate FΔH design limit has to be reduced correspondingly. Such reduction of the FΔH design limit is very demanding for core design and expensive in terms of fuel consumption and might even call for operation at reduced power.

5.2. Thermal-hydraulic water gap penalties

The fuel rods with increased water gaps and moderation, and thereby increased power, also experience improved cooling. Taking this effect into account, the thermal-hydraulic FΔH peaking factor penalty to be accounted for in DNB analyses – performed with a uniform, nominal gap distribution – can be reduced considerably [5]. This means that the peaking factor penalties are not as limiting for DNB analyses as for LOCA analyses, where the full neutronic water gap penalty has to be taken into account, since possible improved cooling also under LOCA conditions is not currently possible to credit.

5.3. Incore water gap penalties

During the monthly flux-mapping for peaking factor verification, traversing incore probes are inserted in the central instrumentation tube of fuel assemblies. The neutron flux registered by these neutron detectors is a function of the fission rate only in the surrounding few rows of fuel rods. The increase in power in the outermost rows of fuel rods, where the water gap effects can be significant, cannot be detected. The water gap effect is only detected to the extent that it affects the quadrant tilt and fuel assembly power. Thus, an incore FΔH peaking factor penalty has to be applied to flux-map results, in order to account for the part of the neutronic penalty which cannot be measured.

In order to encompass an incore FΔH peaking factor penalty within the FΔH core operational limit, the best estimate FΔH design limit has to be reduced correspondingly. In the case of Ringhals 3 and 4, the LOCA aspect is however more limiting for core design.

5.4. Water gap prediction

So far Vattenfall has relied on generic analyses of the water gap peaking factor penalties. An in-house capability to analyze the water gap effects on a cycle-specific basis would be desirable for increased flexibility. This could enable us to optimize core designs with respect to water gap impacts on in-core quadrant power tilt and peaking factors and could also potentially justify a cycle-specific reduction of the peaking factor penalties.

Sophisticated neutronic assembly bow models are present in the SIMULATE-5 3D core simulator used by Vattenfall [6]. In order to routinely perform best estimate water gap analyses, it is necessary to define realistic water gaps distributions to be input to the core model. Using available full-core measurement data, it is possible to calculate the BOC and EOC water gaps.

The out-of-core measured bow amplitudes and shapes at EOC fit well with each other if "re-loaded" into the core as they were loaded during the previous cycle. This indicates that little or no remaining elastic deformations of the assemblies are present at EOC. The permanent deformation out-of-core can be assumed to be the same in-core (not considering friction effects), thus the water gaps can easily be calculated directly from measured out-of-core bow and core geometry data including thermal expansion and grid growth effects. Vattenfall compared water gap distributions calculated with this simplified approach with those calculated with a sophisticated mechanical core model. The comparison confirmed that this simplified approach produces useful results.

Out-of-core measured bow amplitudes and shapes at EOC for fuel assemblies that are reloaded into the next BOC core in a new loading pattern including fresh (straight) fuel assemblies obviously won't fit well with each other, so there will be many interactions between the assemblies. A mechanical model is necessary to determine a new equilibrium state in each core row and column. A simple elastic model for this can be assumed, only taking into account original out-of-core bow shapes and the estimated lateral stiffness of fresh and burnt fuel assemblies, respectively. Vattenfall compared BOC water gaps distributions calculated with this simplified approach with those calculated with a more sophisticated mechanical core model. The comparison shows that the simplified approach agreed reasonably well.

Realistic water gaps calculated from full-core measurement data may be used in the SIMULATE-5 core models for Ringhals 3 and 4, for future cycle-specific evaluations.

6. Conclusion

Fuel assembly bow remains a major concern for Ringhals PWR's. The development of the assembly bow is monitored with annual measurements during outage. In the last 5-6 years, bow measurements in Ringhals 3 and 4 have revealed a transition from relatively minor S-shaped bows with a major bow direction to South-East to increasing amplitudes of C-shaped bows to the North-West.

To improve the understanding of this development a new measurement device, Mabema Fuel 3D, was introduced in 2017 allowing "on-line" full-core bow measurements during core off-loading.

A detailed fuel assembly bow database was built from previous and new bow measurement data. The database enabled tracking relevant bow parameters over time and their possible correlation with other measurement or operational data.

Analysis of the bow data led to the conclusion that the main reason for the development of strong C-bows was the introduction of a new reload fuel design between 2011 and 2012. The transition from S- to C-bow indicated that axial loads are no longer the main driver of bow, but rather the lateral loads from neighbouring, already bowed fuel assemblies and flow forces. Thus, the reload fuel was concluded to provide insufficient lateral stiffness. In cooperation with the fuel vendor, design improvements were implemented and first reloads of the modified product will be loaded in both units in 2018.

The study of full core bow patterns reveals that a "smooth" and symmetric bow pattern with general bow direction towards North-West is recurring at the EOC. The EOC bow amplitude and bow direction of individual assemblies seem to be more dependent on the position in the core/bow pattern, than on other factors including the loading pattern and the number of fresh assemblies. The recurrence of the same bow pattern is partly attributed to the boundary condition imposed by the core baffle, but could hardly occur without the additional aid of lateral flow forces.

Currently a situation close to equilibrium appears to have been reached in Ringhals 3, with a maximum bow, on free-standing assemblies, in the x- or y-direction of around 10 mm. The limited room for bow in the core and the influence of lateral flow forces may explain why the bow development halted. A similar trend is expected to be seen in Ringhals 4. Eventually the introduction of stiffer reload fuel assemblies is expected to reduce the bow amplitudes to a lower equilibrium level.

Investigation of the present bow relative to suggested acceptance criteria shows that Incomplete Rod Insertion is not a real concern for C-shaped bows. C-shaped bows on the other hand have a significant impact on the integral rod power, FΔH, due to the opening up of enhanced water gaps along the length of the fuel assemblies, specifically at BOC with bowed assemblies adjacent to initially straight, fresh fuel assemblies.

Water gap peaking factor penalties are analysed as an integral part of Ringhals safety analysis reports. These water gap analyses had to be revised for Ringhals 3 and 4 in order to cover the effect of C-shaped bow. From a safety analysis perspective, the increased FΔH-penalty is primarily limiting for the LOCA analyses where the full neutronic penalty has to be accounted for, whereas in the DNB analyses it can be shown that a significant part of the penalty from increased power peaking is offset by the improved cooling from the enhanced water gaps.

It seems feasible to use a simplified elastic mechanical model to estimate the water gaps at BOC and EOC based on full-core bow measurement data. We intend to include realistic water gaps in the SIMULATE-5 core models for Ringhals 3 and 4, for cycle-specific evaluations, as a complement to the generic water gaps analyses performed by vendors.

Acknowledgements

The authors gratefully acknowledge the contributions of Mabema AB and the fuel handling group at Ringhals.

References

1. T. Andersson et al., “A Decade of Assembly Bow Management at Ringhals”, Proceedings of the 2004 International Meeting on LWR Fuel Performance, Sep 2004, Paper 1011
2. C. Durand, “Fuel Bowing Performances”, 2017 NEA Workshop: Advanced Fuel Modelling for Safety and Performance Enhancement
3. M. O’Cain et al., “Bow Evaluations to Support Fuel Assembly Design Improvements”, Top Fuel 2018, WAAP-10884, rev. 0
4. R. Fetterman et al., “Analysis of PWR assembly bow”, International Conference on Reactor Physics, Nuclear Power: A Sustainable Resource, Sep 2008
5. R. Mukin et al., “Thermal Hydraulic Analysis of PWR Assembly Bowing Using Subchannel Code COBRA-TF”, NURETH-17
6. M. Kruners, “PWR Bundle Bowing”, Studsvik International Users Group Meeting, Jun 2015